Colloids and Surfaces B: Biointerfaces 144 (2016) 108–117

Contents lists available at ScienceDirect

Colloids and Surfaces B: Biointerfaces

journal homepage: www.elsevier.com/locate/colsurfb

# Fabrication and characterization of vitamin B5 loaded poly (L-lactide-co-caprolactone)/silk fiber aligned electrospun nanofibers for schwann cell proliferation

M. Aqeel Bhutto[a], Tong Wu[a], Binbin Sun[a], Hany EI-Hamshary[b,c], Salem S. Al-Deyab[b], Xiumei Mo[a,b,*]

[a] Biomaterials and Tissue Engineering Lab, College of Chemistry, Chemical Engineering & Biotechnology, Donghua University, Shanghai 201620, PR China
[b] Department of Chemistry, College of Science, King Saud University, Riyadh 11451, Saudi Arabia
[c] Department of Chemistry, Faculty of Science, Tanta University, Tanta 31527, Egypt

ARTICLE INFO

*Article history:*
Received 29 October 2015
Received in revised form 6 April 2016
Accepted 7 April 2016
Available online 7 April 2016

*Keywords:*
Electrospinning
Vitamin B5
P (LLA-CL)
Schwann cells

ABSTRACT

Bioengineering strategies for peripheral nerve regeneration have been focusing on the development of alternative treatments for nerve repair. In present study we have blended the Vitamin B5 (50 mg) with 8% P(LLA-CL) and P(LLA-CL)/SF solutions and produced aligned electrospun nanofiber mashes and characterized the material for its physiochemical and mechanical characteristics. The vitamin loaded composites nanofibers showed tensile strength of $8.73 \pm 1.38$ and $8.4 \pm 1.37$ in P(LLA-CL)/Vt and P(LLA-CL)/SF/Vt nanofibers mashes, respectively. By the addition of vitamin B5 the P(LLA-CL) nanofibers become hydrophilic and the contact angle decreased from 96° to 0° in 6 min of duration. The effect of vitamin B5 on Schwann cells proliferation and viability were analyzed by using MTT assay and the number of cells cultured on vitamin loaded nanofiber mashes was significantly higher than the without vitamin loaded nanofiber samples after 5th day ($p < 0.05$) whereas, P (LLA-CL)/SF/Vt exhibit the consistently highest cell numbers after 7th days culture as compare to P (LLA-CL)/Vt. The in vitro vitamin release behavior was observed in PBS solution and released vitamin was calculated by revers phase HPLC method. The sustain release behavior of vitamin B5 were noted higher in P(LLA-CL)/Vt (80%) nanofibers as compared to P (LLA-CL)/SF/Vt (62%) nanofibers after 24 h. The present work provided a basis for further studies of this novel aligned nanofibrous material in nerve tissue repair or regeneration.



## 1. Introduction

Current bioengineering strategies for peripheral nerve regeneration have been focused on the development of alternative treatments for nerve repair [1]. Recent nanomaterial based scaffolds are produced by combination of various biological molecules such as growth factors, proteins and polysaccharides with natural or synthetic polymers to improve their physiochemical and mechanical properties [2]. Different methods have been used to produce nanostructured scaffolds such as electrospinning [3], phase separation [4], self-assembly [5] and computer aided design based fabrication techniques [6] intended to enhance axonal growth. Nanofibrous scaffolds produced by electrospinning have gained increasing popularity in the field of tissue engineering because of its simplicity and flexibility of processing [7–9]. The basic setup of electrospinning consists of a spinneret, collector and high voltage supply [10]. During electrospinning process high voltage interacts with polymer solution resulting stretch droplet is formed that erupt from the needle tip where sufficient high molecular cohesion produces jet. The elongation of jet is further proceeded by whipping process initiated due to electrostatic repulsion at small bends in the fiber till final deposition to collector [11]. The fiber diameter size depends on the voltage supply, distance between the collector & needle, flow rate and concentration of the solution [12]. We can electrospun wide range of natural or synthetic polymers and even mixed solutions, according to its application in tissue engineering. An electrospun scaffold has characteristic advantages of an extremely high porosity and surface area to volume ratio mimicking the features of extracellular matrix (ECM) and makes it promising for tissue regeneration. Aligned nanofibers have been

* Corresponding author at: Biomaterials and Tissue Engineering Lab, College of Chemistry, Chemical Engineering & Biotechnology, Donghua University, Shanghai 201620, PR China.
*E-mail address:* xmm@dhu.edu.cn (X. Mo).

http://dx.doi.org/10.1016/j.colsurfb.2016.04.013
0927-7765/

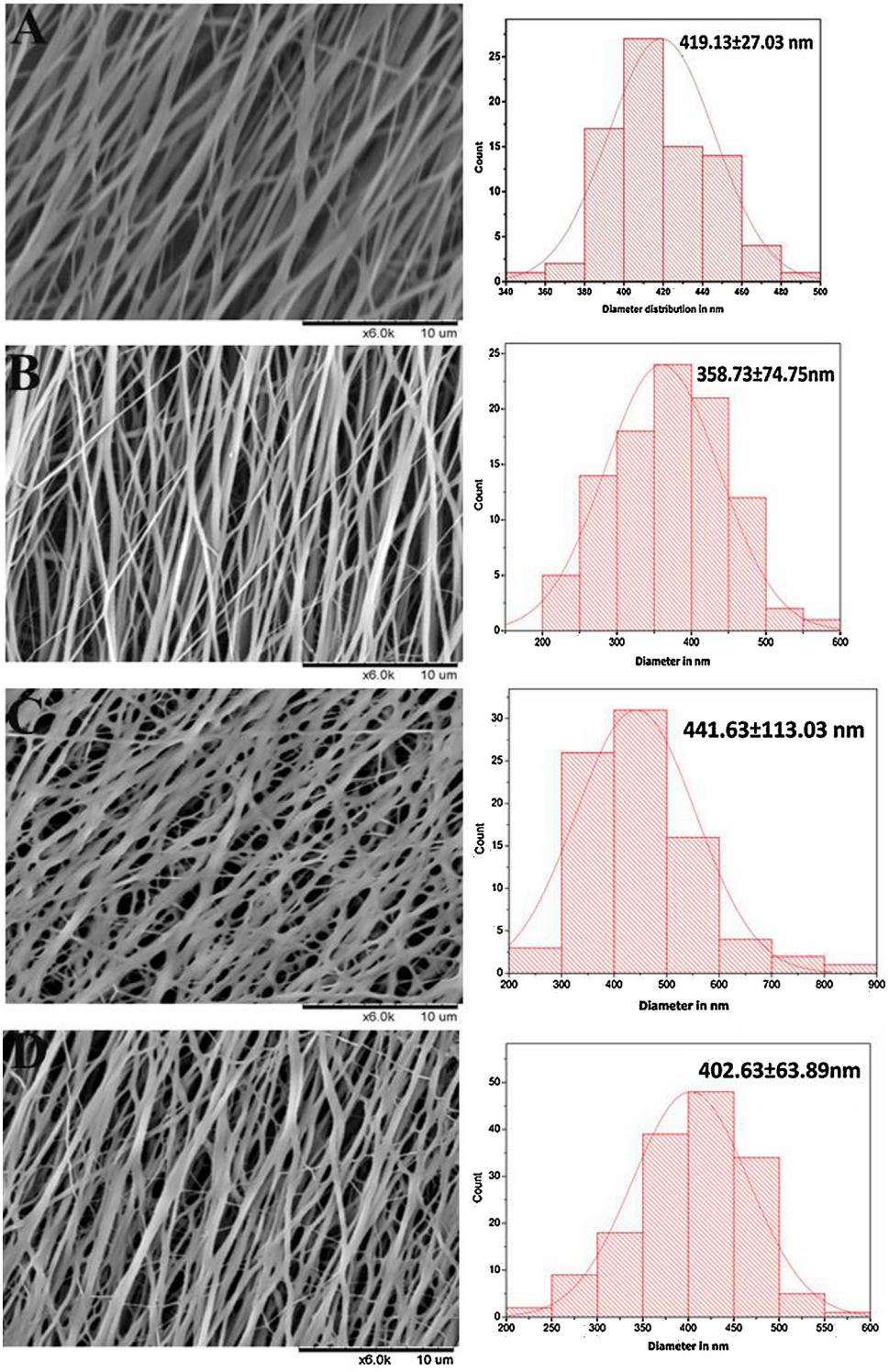


**Fig. 1.** SEM images of nanofibers and their diameter distribution in nm. **A**: P(LLA-CL) **B**: P(LLA-CL)/SF **C**: P(LLA-CL)/Vt **D**: P(LLA-CL)/SF/Vt.

shown to direct cell migration, which plays a critical role in nerve regeneration [13,14]. Aligned nanofibers can be obtained by correct choice of collector in the electrospinning equipment [15]. A number of synthetic or natural biopolymers, such as poly (L-lactic acid) (PLLA), Poly (lactic-co-glycolic acid) (PLGA), Poly (caprolactone) (PCL) collagen and chitosan have been utilized to produce nerve guidance conduit (NGC) for nerve repair [6,16–18]. Although these degradable biomaterials have achieved some encouraging results in neural regeneration but still lacking biological or mechanical properties [19]. Most of the synthetic biodegradable materials have hydrophobic nature which limits their use as tissue engineering scaffolds. The surface hydrophilicity could be enhanced by coating of ECM proteins or specific amino acid sequence on the surface of material by using appropriate surface modification method [20]. Recently some micronutrients such as growth factors, vitamins and other biological molecules are also incorporated in composite manner to enhance the regeneration process in tissue engineering [21–24].

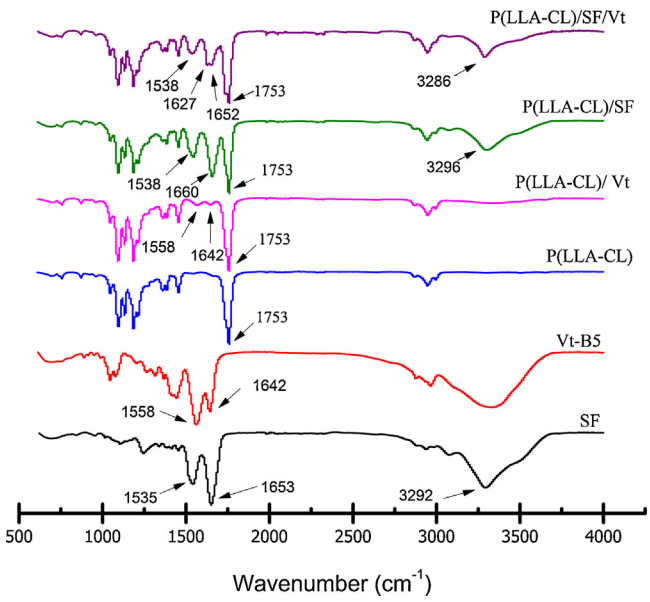


**Fig. 2.** The ATR-FTIR spectrum of SF, Vitamin B5, P(LLA-CL), P(LLA-CL)/Vt, P(LLA-CL)/SF and P(LLA-CL)/SF/Vt.

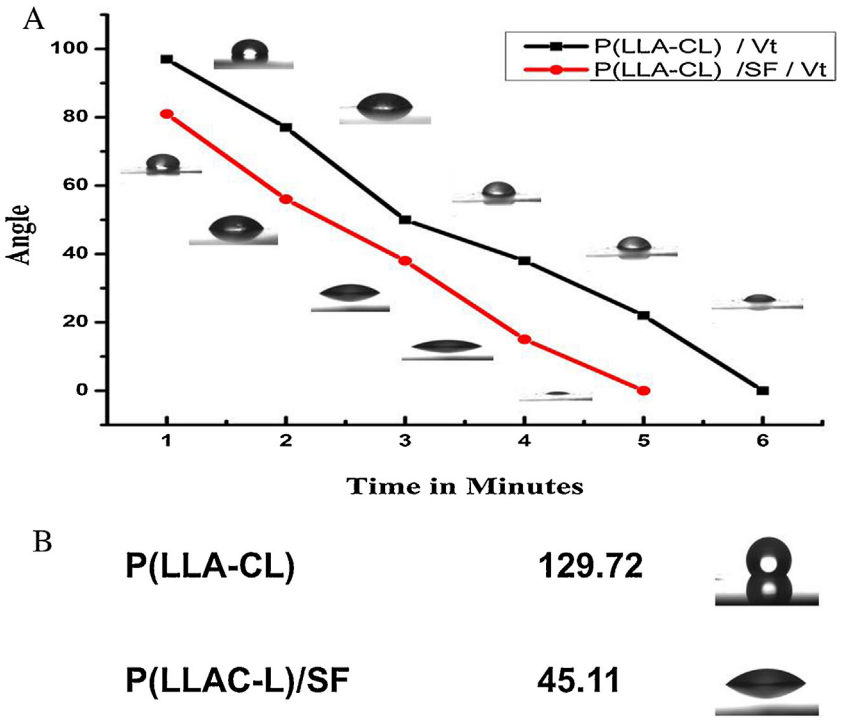


**Fig. 3.** Water contact angle measurement on electrospun nanofibers surface of P(LLA-CL), P(LLA-CL)/SF, P(LLA-CL)/Vt and P(LLA-CL)/SF/Vt.

Vitamins are essential micronutrients and performed various biochemical functions in our body, such as function as hormones, antioxidants, mediators for cell signaling and as regulators of cells or tissue growth and differentiation. Vitamin $B_5$ is water soluble in nature and involve in a variety of reactions that sustain life. Vitamin $B_5$ is part of the B-complex family of vitamins, also known as pantothenic acid or pantothenate. Pantothenic acid is the amide between pantoic acid and β-alanine. It is a component of an essential coenzyme A (CoA), which is necessary for energy metabolism and allowing carbohydrates, fats, and proteins to be burned as fuel source to help mitochondria for its optimal function [25,26]. Meanwhile, Vitamin $B_5$ also supports in the production of acetylcholine, which is a neurotransmitter [27], So incorporation of vitamin B5 as biomaterial in nerve scaffolds could improve the physiochemical properties of nanofiber and may helpful for nerve regeneration.

Previously our group has been reported the well-blended natural-synthetic polymeric electrospun nanofibers of silk fibroin (SF) with poly (L-lactic acid-co-ϵ-caprolactone) (P(LLA-CL)) and it was noted that SF blending with P(LLA-CL) has greatly improved the cell affinity [28]. Further in vivo effect of aligned SF/P(LLA-CL) NGC was studied in the rat sciatic nerve injury model [29]. SF is an excellent biopolymer with diverse properties including good biocompatibility, blood compatibility, good oxygen & water permeability, biodegradability and minimal inflammatory reaction [30,31]. Present work is the continuity of previous work to enhance the efficiency of nerve scaffold, so we blended the Vita-

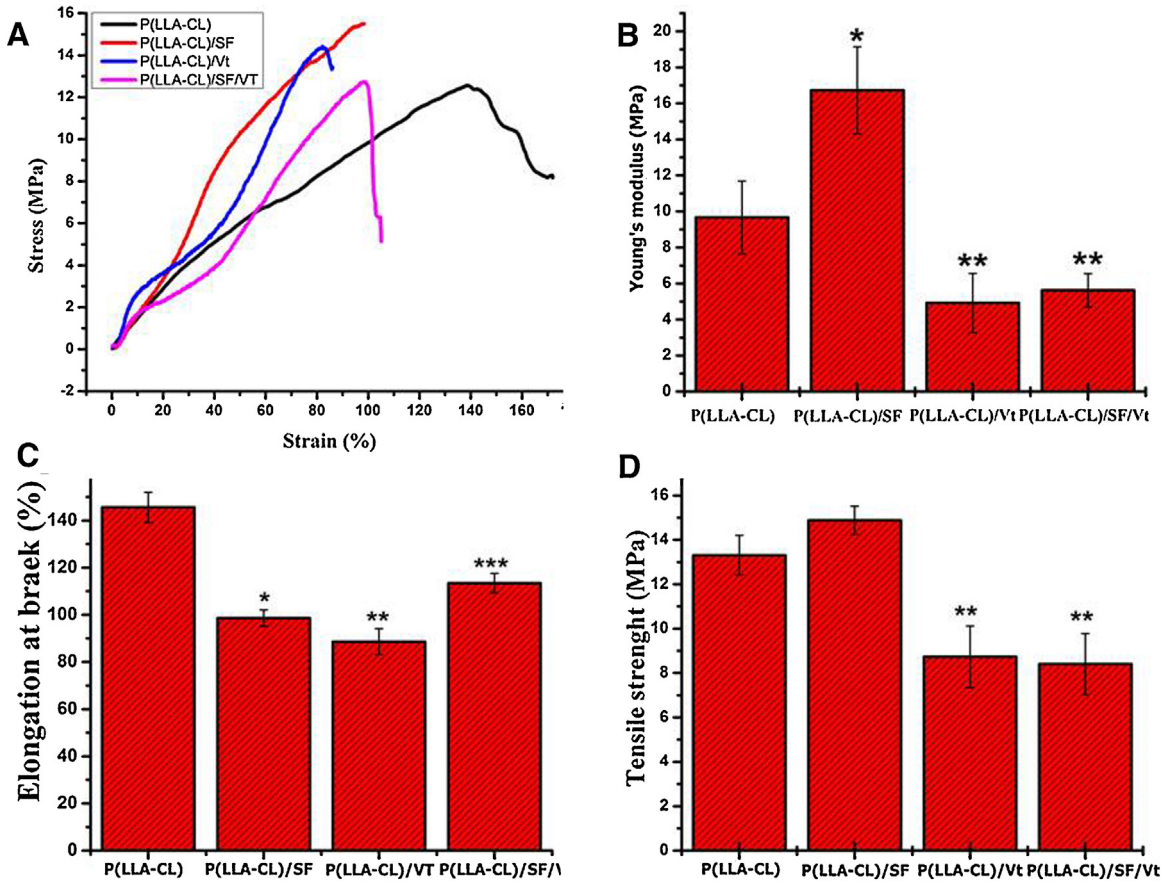


**Fig. 4.** Mechanical properties of nanofibers **A**:tensile stress-strain curve, **B**: tensile strength at break, **C**: elongation at break and **D:** Young's modulus (* = significance difference in comparison with P(LLA-CL),** = P(LLA-CL) and P(LLA-CL)/SF and *** = P(LLA-CL), P(LLA-CL)/SF and P(LLA-CL)/SF/Vt. $p < 0.05$, n = 5).

min $B_5$ with P(LLA-CL) and P(LLA-CL)/SF solutions and produced aligned electrospun nanofiber mashes and characterized the material for its morphology by SEM, FTIR analysis, mechanical strength, and surface wettability properties. The quantitative release behavior of vitamin $B_5$ from loaded nanofibers were determined by HPLC method and evaluated its possible use for nerve tissue engineering by growing of schwann cells and measured its growth by 3-(4,5-dimethylthiazol-2-yl)-2,5-diphenyltetrazolium bromide (MTT) assay. The present work provides basis for further studies of this novel aligned nanofibrous material in nerve tissue repair or regeneration.

## 2. Material and method

### 2.1. Materials

Cocoons of Bombyx mori silkworm were kindly supplied by Jiaxing Silk Co.Ltd. (China), Vitamin $B_5$ were purchased from Sigma. The co-polymer of Poly (L-lactide-co-caprolactone) (P(LLA-CL)) (50:50) was purchased from Jinan Daigang Bioengineering Co. Ltd (China). 1,1,1,3,3,3,-hexafluoro-2-propanol (HFIP) was purchased from Daikin Industries Ltd (Japan). Cell culture reagents including fetal bovine serum (FBS), horse serum (HS), Dulbecco's modified Eagle's medium (DMEM), phosphate-buffered saline (PBS), trypsin/EDTA, RPMI 1640 medium and penicillin–streptomycin were purchased from Invitrogen and Sigma–Aldrich (St. Louis, MO). The Mouse Schwann cells for in vitro analysis were obtained from Shanghai Institute of Biochemistry and Cell Biology (SIBCB, CAS, China).

### 2.2. Preparation of silk fibroin (SF)

The silk fibroin (SF) was prepared as an earlier published procedure [29]. Briefly, raw silk was degummed three times with 0.5 wt% $Na_2CO_3$ solution at 100 °C for 30 min and washed with distilled water. Then degummed silk was dissolved in $CaCl_2/H_2O$/EtOH solution (molar ratio 1:8:2) at 70 °C for 1 h. The solution was dialyzed with cellulose tube (250-7u; Sigma) in distilled water for 3 days at room temperature. The water was exchanged after every 4 h. Finally the SF solution was filtered and freezing-dried to obtain the regenerated SF sponges.

### 2.3. Electrospinning

The electrospinning solution was prepared by dissolving the P(LLA-CL) and silk fibroin with ratio of 70:30 in 1,1,1,3,3,3-Hexafluoro-2-propanol (HFIP) to yield an ultimate concentration of 8 wt% (w/v) and for control pure 8 wt% (w/v) P(LLA-CL) solutions was prepared by using same solvent system. However 50 mg of vitamin $B_5$ were added in both solutions with total volume of 10 mL to produce the P(LLA-CL)/Vt and P(LLA-CL)/SF/Vt solutions, and all prepared solutions were constantly stirred overnight.

The 3 mL of each solution were pumped through 21 gauge needle with the flow rate of 1 mL/hour whereas the distance between the collector and syringe was set 15 cm. A high voltage of 12 KV was supplied by a high voltage power supply (BGG6-358, BMEI Co Ltd, Beijing China). The aligned nanofibers were collected by using the rotating drum collector at a speed of 3000 rpm.

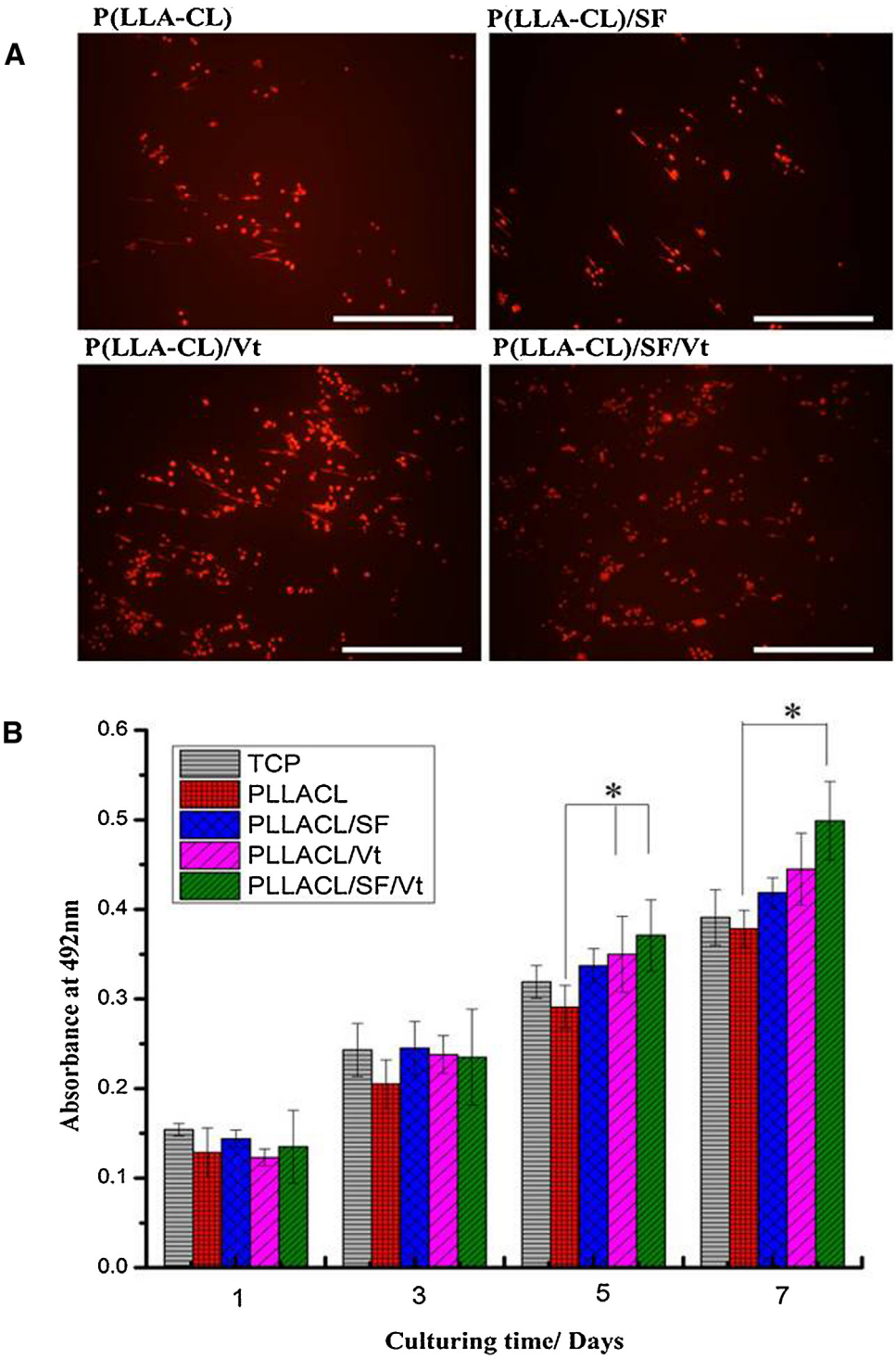


**Fig. 5.** Schwann cell proliferation on P(LLA-CL), P(LLA-CL)/SF, and P(LLA-CL)/Vt and P(LLA-CL)/SF/Vt nanofibers. **A**: Phalloidin staining (scale bar 200um), **B**: MTT assay. (* = significance difference; $p < 0.05$ n = 3).

### 2.4. Morphology of electrospun nanofibers

The structure and surface morphology of the prepared nanofibers were observed by scanning electron microscope (SEM) [32]. Dry samples were sputter-coated with gold for 10 s (twice) before the scanning of SEM at the accelerating voltage of 10 kV. Finally according to SEM Image 100 nanofibers were selected randomly, measured and contrasted them by using Image J software (National Institute of Health, USA), then calculated the average diameter distribution and fiber diameter of the electrospun nanofibers.

### 2.5. Characterization of electrospun nanofibers

The characterization of prepared scaffold was evaluated by Fourier transforms infrared spectroscopy (ART-FTIR) as reported earlier [33]. Infrared measurements were recorded for each sample on an Avatar 380 FTIR spectrometer (Nicolet 6700, Thermo Fisher,

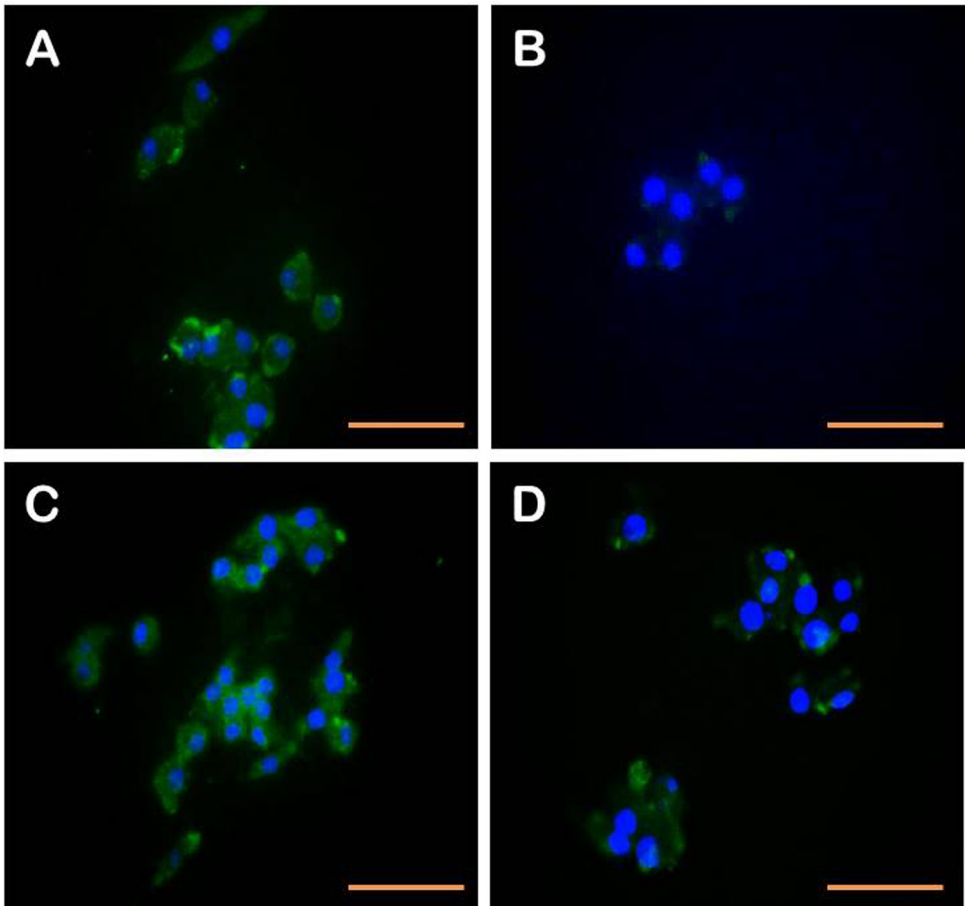


**Fig. 6.** Fluorescent images of Schwann cells cultured on the surface of aligned nanofibers with labeling of cytoplasm (green) and nuclei (blue).**A**: P(LLA-CL), **B:** P(LLA-CL)/Vt, **C**: P(LLA-CL)/SF and **D**: P(LLA-CL)/SF/Vt. (Scale bar = 100 μm). (For interpretation of the references to colour in this figure legend, the reader is referred to the web version of this article.)

USA) at transmission mode (32 scans) in the wavelength ranges of 500–4000 $cm^{-1}$. The water contact angle measurements were tested to find the surface wettability properties of material by using a contact angle measurement instrument (OCA40, Dataphysics, Germany). 0.3 mL deionized water was used for each measurement and 5 different positions on each sample were averaged.

The mechanical strength of the electrospun samples ($10 \times 30\ mm^2$, n = 5) were tested by universal material tester (H5 K-S, Hounsfield,UK) at an ambient temperature of 20 °C with 65% humid environment. The cross head speed was set at 10 mm/min, and the stress-strain curves were calculated for each sample. Finally tensile strength, elongation and young's modulus were calculated.

### 2.6. Cell culture and seeding

Mouse Schwann cells (Chinese Academy of Sciences, Shanghai, China) were cultured in Alpha Minimum Essential Medium containing 10% fetal bovine serum and 1% streptomycin/penicillin and maintained at 37 °C in a $CO_2$ incubator. The media were changed on every 2nd day. The scaffolds were cut to 14 mm diameter and placed into 24-well plates and triplicate samples were used for each scaffold. The samples were sterilized with 75% ethanol for 2 h, then washed with PBS and soaked in cell culture medium for overnight. Schwann cells were then seeded at a density of $1.0 \times 10^4$ cells per well and cultured for a period of 7 days.

### 2.7. Cell proliferation and morphology on scaffolds

The experiment of MTT measured the cell proliferation and viability was performed at 1, 3, 5 and 7 day of post-seeding, respectively. Each test point has performed three parallel experiments. The plate was read at the absorbance of 492 nm using an enzyme-labeled instrument (MK3, Thermo, USA). The results of experimental data was analysis by origin 7.5, T-test were also conducted to find out the salient differences of cell proliferation in different scaffolds.

Cell proliferation and morphology were studies on the different scaffolds by performing paraffin embedding phalloidin and Immunofluorescence staining. After 4 days of post-seeding, cell-scaffolds were removed form media and rinsed thricely with PBS (5 min per wash) and fixed with 4% (v/v) paraformaldehyde solution for 30 min, washed with PBS to remove non-adherent cells, permeabilized in 0.1% Triton X-100 for 6 min, and then blocked in 1% BSA for 30 min and stained with phalloidin. Immunofluorescence staining was performed as described earlier [34], samples were blocked in 10% normal serum with 1% BSA in TBS for 2 h at room temperature then S-100 (ab4066-Abcam) applied as primary antibody diluted in TBS with 1% BSA and incubated overnight at 4 °C. After overnight incubation samples were rinsed thricely with TBS 0.025% Triton and incubated for 1 h with conjugated Goat Anti-mouse IgG (H + L) CY3 (GB21301- Abcam) diluted as per recommended concentration by manufacturer. Counter stained with DAPI after rinsing the scaffolds with TBS and cell proliferation was observed under an optical microscope (H600L, Nikon, Japan).

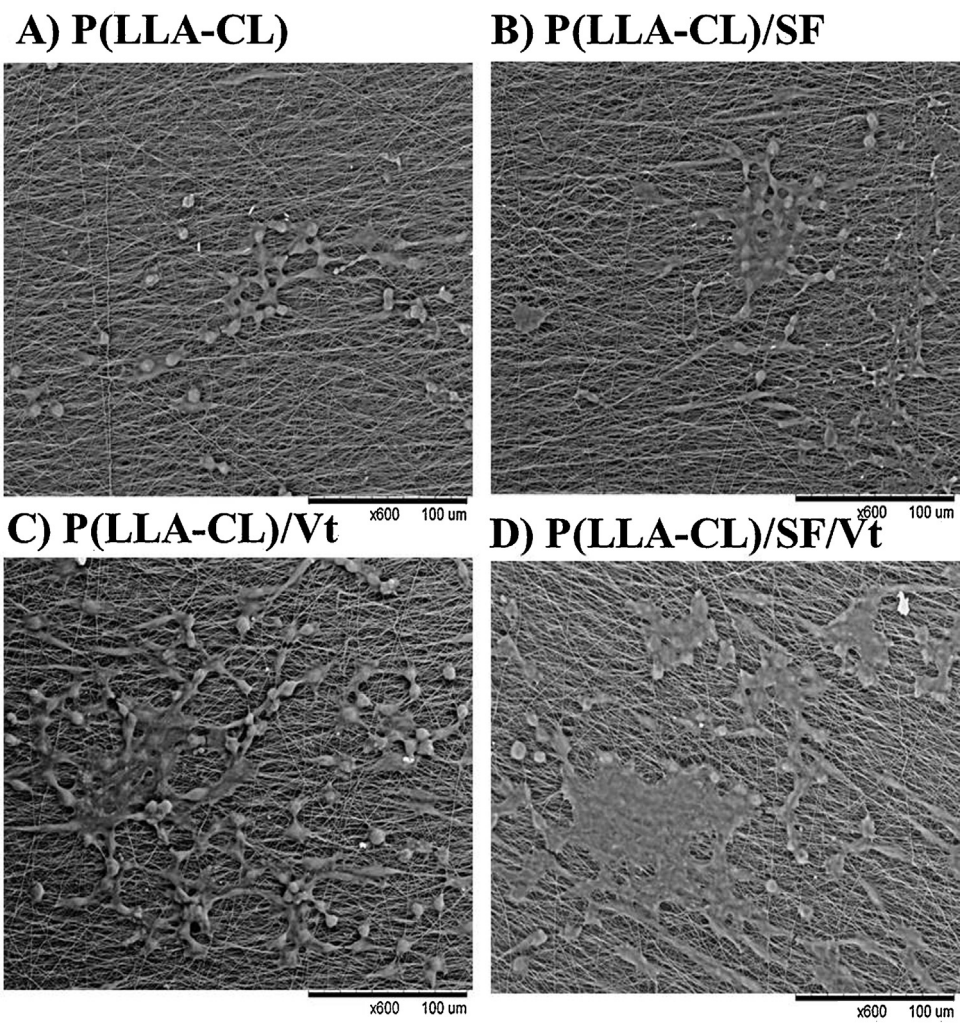


**Fig. 7.** SEM images of Schwann cell growth on P(LLA-CL) and P(LLA-CL)/SF nanofibers with and without vitamin B5.

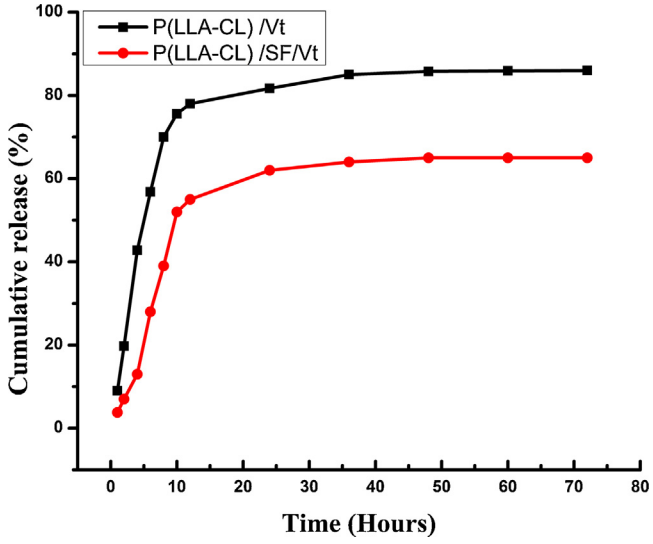


**Fig. 8.** In vitro release of vitamin B5 from P(LLA-CL)/Vt and P(LLA-CL)/SF/Vt nanofibrous mats.

Cell morphology and the interaction between cells and scaffolds were also studied by SEM at 4th day of incubation. The scaffolds were removed from culture media and gently washed with PBS then cells were fixed with 4% (v/v) paraformaldehyde solution for 30 min at 4 °C. The scaffolds were dehydrated with different ethanol concentrations of 30, 50, 70, 90 and 100% (v/v) respectively before being dried. Subsequently samples were coated with gold for 10 s

(twice) at the accelerating voltage of 10 kV and then imaged via SEM.

### 2.8. In vitro vitamin $B_5$ release studies

The release profile of vitamin $B_5$ loaded P(LLA-CL)/Vt and P(LLA-CL)/SF/Vt nanofibers were investigated in PBS at pH 7.4. All samples (2 × 2 cm) were incubated at 37 °C in 10 mL of the aforementioned release medium under stirring condition. Aliquots of samples (1 mL) were taken from the release medium after specific time intervals and volume was replaced with fresh PBS. The amount $B_5$ released at various times up to 72 h was determined using a reversed-phase HPLC method [35], consisting of analytical reversed phase C-18 column (XDB-C18, 150 × 4.6 mm, 5 μm, Agilent, USA), while mobile phase consisting of a mixture of buffer and methanol in the ratio of 80:20 (V/V) delivered at the flow rate of 1 mL/min with UV detection at 210 nm. Calibration curve of vitamin $B_5$ measured under the same parameters and the percentage of $B_5$ release was calculated and plotted versus time according to the following equation.

$$\text{Release}\,(\%) = \frac{Release\ B5}{Tatal\ Loaded\ B5} \times 100$$

### 2.9. Statistics analysis

Statistical analysis was performed using 8.0 (Origin Lab Inc.,USA). All the values were in triplicate and expressed as means± standard deviation (SD). Statistical difference between control and different samples was determined via one way ANOVA paired test followed by Bonferroni's multiple comparison test ($p < 0.05$) considered as statistically significant.

## 3. Results and discussion

### 3.1. Morphology of electrospun nanofibers

Fig. 1 showed the morphology and alignments of electrospun nanofibers. SEM images showed that average diameter of P(LLA-CL) nanofiber was 419.13 ± 27.03 nm (Fig. 1A) and P(LLA-CL)/SF was 358.73 ± 74.75 nm (Fig. 1B). However, diameter of the P(LLA-CL)/Vt and P(LLA-CL)/SF/Vt was noted as 441.63 ± 103.03 nm (Fig. 1C) and 402.63 ± 63.89 nm (Fig. 1D) respectively. It was observed that the diameter of P(LLA-CL)/SF nanofibers are smaller than P(LLA-CL) nanofibers as we have previously reported, it may be due to the presence of hydrophilic groups of SF, composed of lager side chains of amino acids which carry repetitive same electric charges, resulting the repulsive force between these same electric charges were increased during the process of electrospinning produced smaller nanofibers of P(LLA-CL)/SF [36]. Meanwhile, by addition of vitamin $B_5$ (50 mg) in both solutions increased nanofiber diameter, it might be due to changing in viscosity of solutions. Previously it is reported that under the same electrospinning parameters if solution concentration is changed it effects on diameter of the nanofibers [37,38].

### 3.2. Characterization of electrospun nanofibers

The chemical characteristics of the electrospun nanofibers were determined by ATR-FTIR spectroscopy. Fig. 2 shows ATR-FTIR spectrum of SF, Vitamin $B_5$, P(LLA-CL), P(LLA-CL)/Vt, P(LLA-CL)/SF and P(LLA-CL)/SF/Vt. The spectra for pure vitamin $B_5$ represents the main characteristic two peaks of amide I ($\nu_{C=O}$) and amide II ($\delta_{NH}$) at 1642 $cm^{-1}$ and 1558 $cm^{-1}$ respectively, whereas P(LLA-CL) spectra imply the characteristic ester group stretching peak at 1753 $cm^{-1}$ (C=O).The appearing of all these three peaks in P(LLA-CL)/Vt nanofiber spectra implying the presence of vitamin with P(LLA-CL). The main characteristic peak of raw SF was noted at 3292 $cm^{-1}$, which represents to N—H and hydroxyl O—H, corresponding of the stretching vibration of free amino acid group. However, the absorbance peak of SF 3292 $cm^{-1}$ is shifted to 3296 $cm^{-1}$ in P(LLA-CL)/SF nanofiber. The absorbance peaks at 1653 $cm^{-1}$ and 1535 $cm^{-1}$ in raw SF are attributed to amide I and amide II respectively [39]. During blending of SF with P(LLA-CL), the characteristic peak of amide I shifted from 1653 $cm^{-1}$ to 1660 $cm^{-1}$,which is attributed to the bond C=N and C—N implied to the crosslinking reaction, However characteristic adsorption peak of amide II 1535 $cm^{-1}$ shifted to 1538 $cm^{-1}$,which represents the transitional change of SF from α-helix to β-sheet structure [28]. By the addition of vitamin with P(LLA-CL)/SF solution the characteristic absorbance peak for vitamin is shifted from 1642 cm to 1627 cm whereas amide II peaks are also shifted from 1535 cm to 1538 $cm^{-1}$ same as in P(LLA-CL)/SF nanofibers but no significance difference were observed in characteristic peak of amide I with reference to raw SF, However the main characteristic peak of SF was also shifted from 3292 $cm^{-1}$ to 3286 $cm^{-1}$.

Surface wettability properties of biomaterials are very important because it influences on cell adhesion, proliferation and migration. The water contact angle measurements on P(LLA-CL) and P(LLA-CL)/SF nanofibers surface with and without vitamin are illustrated in Fig. 3. Results showed that P(LLA-CL) nanofibers surface were hydrophobic (129.72°), However by the addition of water soluble vitamin $B_5$ the nanofibers become hydrophilic and the contact angle decreased from 96° to 0° in 6 min of duration. Meanwhile, P(LLA-CL)/SF nanofibers surface also observed as hydrophilic and contact angle measurement observed to 45.11° in 3 min analysis, whereas, the addition of vitamin initially the fiber surface showed contact angle measurement at 81° which is higher as compared to without vitamin loaded fibers surface but within 5 min it gradually decreased to 0°. These results are confirming that vitamin is present throughout the nanofiber mashes and its water soluble nature turns the hydrophobic P(LLA-CL) fibers into hydrophilic which supports cell attachment and growth.

Mechanical properties of nanofibers play a very critical role in application, as it need to provide an initial biomechanical profile for the cells before new tissue can be formed [40]. The average thickness of P(LLA-CL), P(LLA-CL)/SF, P(LLA-CL)/Vt and P(LLA-CL)/SF/Vt nanofibers meshes were 0.045, 0.0425, 0.05 and 0.05 mm, respectively. The mechanical properties of the P(LLA-CL) and P(LLA-CL)/SF with and without vitamin loaded nanofibers were characterized by tensile measurement. Fig. 4 represents the mechanical parameters of with and without vitamin loaded P(LLA-CL) and P(LLA-CL)/SF electrospun nanofibers, including the stress- strain curve, tensile strength, elongation at break and Young's modulus. As shown in Fig. 4A all samples exhibit a linear elastic behavior. The tensile strength and elongation at break is about two fold higher in P(LLA-CL) and P(LLA-CL)/SF nanofibers as compare to P(LLA-CL)/Vt and P(LLA-CL)/SF/Vt nanofibers. For example, By the addition of vitamin the tensile strength of P(LLA-CL) nanofibers are decrease from 13.31 ±0.89 to 8.73 ± 1.38 MPa in P(LLA-CL)/Vt nanofibers mashes whereas, in P(LLA-CL)/SF nanofibers it decreased from 14.88 ± 0.63 to 8.4 ± 1.37 MPa (Fig. 4D). Meanwhile the elongation at break of P(LLA-CL) nanofibers were noted at 145.61 ± 6.33% which is dropped down to 98.56 ± 3.48% in P(LLA-CL)/SF nanofibers however 88 ± 5.50% and 110 ± 2.1% in P(LLA-CL)/Vt and P(LLA-CL)/SF/Vt nanofibers mashes respectively (Fig. 4C). The young's modulus of P(LLA-CL) nanofibers exhibited the variable trend, increased from 9.66 ± 2.01 to 16.73 ± 2.41 MPa in P(LLA-CL) to P(LLA-CL)/SF nanofibers and by the addition of vitamin decreased to 4.92 ± 1.6 and 5.62 ± 0.93 MPa in P(LLA-CL)/Vt and P(LLA-CL)/SF/Vt nanofibers mashes (Fig. 4B), respectively. Although the value is decreased with the addition of vitamin but still vitamin loaded nanofibers are relative elastic and suitable for nerve tissue engi-

neering, that will be helpful in handling and suturing during implant surgery.

### 3.3. Cell proliferation and morphology on electrospun nanofibers

The cytocompatibility of P(LLA-CL) and P(LLA-CL)/SF have been demonstrated in our previous work. To find the effect of vitamin $B_5$ in nanofibers mat on proliferation and viability of Schwann cells were analyzed by using MTT assay. As shown in Fig. 5B, the number of cells cultured on vitamin loaded nanofiber mashes was significantly higher than the without vitamin loaded nanofiber samples after 7th day ($p < 0.05$) whereas, P(LLA-CL)/SF/Vt exhibit the consistently highest cell numbers after 7th day culture as compare to P(LLA-CL)/Vt. We also investigated morphology and distribution of Schwann cells on aligned nanofibers after 4th days of incubation by phalloidin staining (Fig. 5A). The density of cells cultured on P(LLA-CL)/SF/Vt and P(LLA-CL)/Vt were higher than without vitamin nanofiber mashes of P(LLA-CL) and P(LLA-CL)/SF. This might be because of two reasons, First in vitamin loaded nanofibers the change in surface wettability property (highly hydrophilic) enhances the cell adhesion and proliferation rate and second the liberation of free vitamin in the cell surrounding enhanced the cell activity, literature also reveals that vitamin $B_5$ is helpful in increase of cellular mitochondrial metabolic activity [25,28].

The Schwann cell morphology on nanofibers was studied by immunofluorescence staining (Fig. 6), which expressed cell nuclei with blue colour while fluorescence labeled cell proteins with green colour. It was observed cells have shown good cell interaction on vitamin loaded nanofibers as compared to without loaded vitamin nanofibers. SEM images also reveal the cell–cell and cell-matrix interaction (Fig. 7). Similar enhanced growth behavior of vitamin $B_5$ loaded nanofibers were observed as compared to without vitamin loaded nanofibers mates. Notably on P(LLA-CL) and P(LLA-CL)/SF nanofibers schwann cells grow in dispersed form (in small group), it might be due to hydrophobic nature of nanofibers and resulting cells could not properly adhere the surface whereas on rest of nanofibers mates growth is very smooth and specially on vitamin loaded nanofibers mate the cell grow in high dens and grew well along the direction of nanofibers with oriented cellular morphology, which could plays an important role in rapid filling of gap in nerve regeneration.

### 3.4. In vitro release of vitamin $B_5$ from the nanofibrous mats

Fig. 8 represents the in vitro release profile of vitamin B5 from vitamin loaded P(LLA-CL)/Vt and P(LLA-CL)/SF/Vt nanofibers at various times, up to 72 h, measured using HPLC method. The total loaded vitamin was calculated as 0.815 mg in each sample whereas the recommended nutritional oral dose of vitamin $B_5$ is 5–8 mg per day. P(LLA-CL)/Vt nanofibers shows the initial drug release instantaneously after immersion in PBS was 9% in 1 h, which then showed a burst release in 10 h up to 75%, and then reached a sustain saturation of 80% in 24 h. The final release of hydrophilic vitamin $B_5$ after 3 days treatments with PBS was observed 86%. However, a low percentage vitamin released was noted in P(LLA-CL)/SF/Vt nanofibers which start from 3.8% in 1 h and reached a sustain saturation of 52% in 10 h, than reached a sustain saturation of 62% after 24 h and finally in three days observation it shows parallel and reached to 65%.It is reported that the release mechanism of the drug release behavior could be diffusion, polymer erosion or combination of diffusion and polymer erosion [41]. We believe that the initial burst release and later stable and sustained release behavior of vitamin in this study was caused by the location of vitamin in fibers. It is easy to understand that vitamin located on the fibers surface was easily dissolved in PBS solution at the initial stage. Vitamin B5 is water soluble in nature, which have more charged groups (such as amide I ($\nu_{C=O}$) and amide II ($\delta_{NH}$)) than P (LLA-CL), Therefore, more vitamins compelled to move onto the fiber surface during electrospinning process due to electric force in P(LLA-CL)/Vt nanofibers. However in P(LLA-CL)/SF/Vt nanofibers the presences of vitamin on fiber surface will be low as compared to P (LLA-CL)/Vt because of the presence of charged groups of SF. Therefore, after the initial stage, the vitamin released was sustained and showed stable behavior and the ultimate proportion of released vitamin from P(LLA-CL)/Vt and P(LLA-CL)/SF/Vt nanofibers were closed to 86% and 65% respectively, at the end of three days test.

## 4. Conclusion

In present work we have successfully blended the Vitamin $B_5$ with P(LLA-CL) and P(LLA-CL)/SF solutions to produced aligned electrospun nanofiber mashes with well inherited excellent characteristic of vitamin $B_5$ and SF, encouraging the proliferation of Schwann cells. The vitamin loaded composites nanofibers are relative elastic and suitable for nerve tissue engineering, that will be helpful in handling and suturing during implant surgery. The sustain release behavior of vitamin $B_5$ from loaded nanofibers were implying for its possible use for nerve tissue engineering and other related application. The present work provides a basis for further studies of this novel aligned nanofibrous material in nerve tissue repair or regeneration.

## Acknowledgements

This research was supported by National Nature Science Foundation of China (31470941, 31271035), Science and Technology Commission of Shanghai Municipality (15JC1490100, 15441905100), Ph.D. Programs Foundation of Ministry of Education of China (20130075110005) and light of textile project (J201404), The authors would like to extend their sincere appreciation to the Deanship of Scientific Research at King Saud University for financial support regarding this research group, project no.RGP-201.

## References

[1] C.Y. Wang, et al., The effect of aligned core-shell nanofibres delivering NGF on the promotion of sciatic nerve regeneration, J. Biomater. Sci. Polym. Ed. 23 (1-4) (2012) 167–184.
[2] X. Gu, et al., Construction of tissue engineered nerve grafts and their application in peripheral nerve regeneration, Prog. Neurobiol. 93 (2) (2011) 204–230.
[3] F. Yang, et al., Fabrication of nano-structured porous PLLA scaffold intended for nerve tissue engineering, Biomaterials 25 (10) (2004) 1891–1900.
[4] S. Stokols, M.H. Tuszynski, The fabrication and characterization of linearly oriented nerve guidance scaffolds for spinal cord injury, Biomaterials 25 (27) (2004) 5839–5846.
[5] F. Gelain, L.D. Unsworth, S. Zhang, Slow and sustained release of active cytokines from self-assembling peptide scaffolds, J. Controlled Release 145 (3) (2010) 231–239.
[6] A. Rajaram, X.B. Chen, D.J. Schreyer, Strategic design and recent fabrication techniques for bioengineered tissue scaffolds to improve peripheral nerve regeneration, Tissue Eng. Part B Rev. 18 (6) (2012) 454–467.
[7] W.-E. Teo, W. He, S. Ramakrishna, Electrospun scaffold tailored for tissue-specific extracellular matrix, Biotechnol. J. 1 (9) (2006) 918–929.
[8] J. Xie, X. Li, Y. Xia, Putting electrospun nanofibers to work for biomedical research, Macromol. Rapid Commun. 29 (22) (2008) 1775–1792.
[9] J.D. Schiffman, C.L. Schauer, A review: electrospinning of biopolymer nanofibers and their applications, Polym. Rev. 48 (2) (2008) 317–352.
[10] Q.P. Pham, U. Sharma, A.G. Mikos, Electrospinning of polymeric nanofibers for tissue engineering applications: a review, Tissue Eng. 12 (5) (2006) 1197–1211.
[11] D. Li, Y. Xia, Electrospinning of nanofibers: reinventing the wheel? Adv. Mater. 16 (14) (2004) 1151–1170.
[12] N. Ketabchi, et al., Preparation and optimization of chitosan/polyethylene oxide nanofiber diameter using artificial neural networks, Neural Comput. Appl. (2016).
[13] Y. Chew Sing, et al., The effect of the alignment of electrospun fibrous scaffolds on Schwann cell maturation, Biomaterials 29 (6) (2008) 653–661.

[14] J. Venugopal, et al., Interaction of cells and nanofiber scaffolds in tissue engineering, J. Biomed. Mater. Res. Part B-Appl. Biomater. 84B (1) (2008) 34–48.
[15] F. Zamani, et al., Effects of PLGA nanofibrous scaffolds structure on nerve cell directional proliferation and morphology, Fibers Polym. 14 (5) (2013) 698–702.
[16] T.B. Bini, et al., Electrospun poly(L-lactide-co-glycolide) biodegradable polymer nanofibre tubes for peripheral nerve regeneration, Nanotechnology 15 (11) (2004) 1459–1464.
[17] R.V. Bellamkonda, Peripheral nerve regeneration: an opinion on channels, scaffolds and anisotropy, Biomaterials 27 (19) (2006) 3515–3518.
[18] G. Ciardelli, V. Chiono, Materials for peripheral nerve regeneration, Macromol. Biosci. 6 (1) (2006) 13–26.
[19] N. Bhattarai, et al., Natural-synthetic polyblend nanofibers for biomedical applications, Adv. Mater. 21 (27) (2009) (2792-+).
[20] A. Subramanian, U.M. Krishnan, S. Sethuraman, Development of biomaterial scaffold for nerve tissue engineering: biomaterial mediated neural regeneration, J. Biomed. Sci. 16 (2009) 108.
[21] X. Sheng, et al., Vitamin E-loaded silk fibroin nanofibrous mats fabricated by green process for skin care application, Int. J. Biol. Macromol. 56 (0) (2013) 49–56.
[22] C. He, et al., Fabrication of fibrinogen/P(LLA-cL) hybrid nanofibrous scaffold for potential soft tissue engineering applications, J. Biomed. Mater. Res. A 97 (3) (2011) 339–347.
[23] Y. Xu, et al., The effect of mechanical stimulation on the maturation of TDSCs-poly(L-lactide-co-e-caprolactone)/collagen scaffold constructs for tendon tissue engineering, Biomaterials 35 (9) (2014) 2760–2772.
[24] Z. Kuihua, et al., Aligned SF/P(LLA-cL)-blended nanofibers encapsulating nerve growth factor for peripheral nerve regeneration, J. Biomed. Mater. Res. A 102 (8) (2014) 2680–2691.
[25] L.R. Engelking, Chapter 41 – Niacin (B3) and pantothenic acid (B5), in: L.R. Engelking (Ed.), Textbook of Veterinary Physiological Chemistry, 3rd edn., Academic Press, Boston, 2015, pp. 265–270.
[26] D. Nohr, H.K. Biesalski, E.I. Back, Vitamins | Pantothenic Acid, in Encyclopedia of Dairy Sciences, in: J.W. Fuquay (Ed.), 2nd edn., Academic Press, San Diego, 2011, pp. 694–696.
[27] O.W. Richard, The stimulation of yeast proliferation by pantothenic acid, J. Biol. Chem. 113 (02) (1935) 531–536.
[28] K. Zhang, et al., Fabrication of silk fibroin blended P(LLA-cL) nanofibrous scaffolds for tissue engineering, J. Biomed. Mater. Res. A 93A (3) (2010) 984–993.
[29] W. Chun-Yang, et al., Aligned natural-synthetic polyblend nanofibers for peripheral nerve regeneration, Acta Biomater. 7 (2) (2011) 634–643.
[30] C. Vepari, D.L. Kaplan, Silk as a biomaterial, Prog. Polym. Sci. 32 (8-9) (2007) 991–1007.
[31] W.H. Park, et al., Effect of chitosan on morphology and conformation of electrospun silk fibroin nanofibers, Polymer 45 (21) (2004) 7151–7157.
[32] M.A. Bhutto, et al., Development of poly (L-lactide-co-caprolactone) multichannel nerve conduit with aligned electrospun nanofibers for Schwann cell proliferation, Int. J. Polym. Mater. Polym. Biomater. 65 (7) (2016) 323–329.
[33] B. Sun, et al., Fabrication and characterization of mineralized P(LLA-cL)/SF three-dimensional nanoyarn scaffolds, Iran. Polym. J. 24 (1) (2014) 29–40.
[34] K. Tomita, et al., Effects of the in vivo predegenerated nerve graft on early Schwann cell migration: quantitative analysis using S100-GFP mice, Neurosci. Lett. 461 (1) (2009) 36–40.
[35] M.N. Hasan, M. Akhtaruzzaman, M.Z. Sultan, Estimation of vitamins B-complex (B2: B3, B5 and B6) of some leafy vegetables indigenous to Bangladesh by HPLC method journal of analytical sciences, Methods and Instrum. 03 (03) (2013) 24–29.
[36] C.Y. Wang, et al., Aligned natural-synthetic polyblend nanofibers for peripheral nerve regeneration, Acta Biomater. 7 (2) (2011) 634–643.
[37] Y. Zhu, et al., Stable: superhydrophobic, and conductive Polyaniline/Polystyrene films for corrosive environments, Adv. Funct. Mater. 16 (4) (2006) 568–574.
[38] I. Jun, S. Jeong, H. Shin, The stimulation of myoblast differentiation by electrically conductive sub-micron fibers, Biomaterials 30 (11) (2009) 2038–2047.
[39] M. Farokhi, et al., Structural and functional changes of silk fibroin scaffold due to hydrolytic degradation, J. Appl. Polym. Sci. 131 (6) (2014) n/a–n/a.
[40] Z.G. Chen, et al., Electrospun collagen-chitosan nanofiber: a biomimetic extracellular matrix for endothelial cell and smooth muscle cell, Acta Biomater. 6 (2) (2010) 372–382.
[41] Y. Dong, Z. Zhang, S.S. Feng, D-alpha-tocopheryl polyethylene glycol 1000 succinate (TPGS) modified poly(l-lactide) (PLLA) films for localized delivery of paclitaxel, Int. J. Pharm. 350 (1-2) (2008) 166–171.